Biophysical Chemistry 27 (1987) 15–25
Elsevier

BPC 01129

Kinetic study of the transient phase of a chemical reaction system coupled to an enzymatically catalyzed step

Application to the oxidation of epinine by tyrosinase

Josefa Escribano [a], Manuela García [b], Francisco García Cánovas [a], Francisco García Carmona [c], Ramón Varón [b], José Tudela [a] and J.A. Lozano [a]

[a] *Departamento de Bioquímica, Facultad de Medicina, Universidad de Murcia,* [b] *Cátedra de Química I, Escuela Universitaria Politécnica, Universidad de Castilla-La Mancha and* [c] *Departamento de Bioquímica, Facultad de Biología, Universidad de Murcia, Murcia, Spain*

Received 21 August 1986
Revised manuscript received 30 December 1986
Accepted 13 January 1987

Enzyme kinetics; Transient phase; Tyrosinase; Catecholamine; Adrenergic drug; Deoxyepinephrine

The present work deals with epinine oxidation by mushroom tyrosinase and sodium metaperiodate. Intermediates produced within short reaction times were characterized by repetitive scanning spectrophotometry and the stoichiometry of the appearance of the respective aminochrome was established. The oxidation pathway from epinine to aminochrome had the following steps: epinine → *o*-quinone-H^+ → *o*-quinone → leukoaminochrome → aminochrome. The stoichiometry for the conversion of *o*-quinone-H^+ into the aminochrome of epinine followed the equation: 2 *o*-quinone-H^+ → epinine + aminochrome. A transient phase kinetic study has been developed for the system of chemical reactions coupled to an enzymatically catalyzed step, these taking place when epinine is oxidized by mushroom tyrosinase. Rate constants for the implied chemical steps at different temperature and pH values were calculated from analysis of the progress curves of aminochrome accumulation with time. The thermodynamic activation parameters of the chemical steps were also calculated.

1. Introduction

There is evidence suggesting that oxidation and polymerization systems in melanogenesis are not strictly specific to L-tyrosine and L-dopa, the precursors of melanin biosynthesis in skin and hair of mammals [1]. Moreover, the possibility of a minority metabolic pathway for adrenergic drugs has been proposed [2].

We have previously studied L-dopa oxidation to dopachrome catalyzed by tyrosinase [3,4], extending our study to adrenergic drugs [5–8]. In these studies, using spectrophotometry, the routes of oxidation by tyrosinase of the above compounds were established from measurements vs. time of the appearance of the first steady product of the system, the aminochrome. Furthermore, the values of the deprotonation and cyclization constants of the corresponding *o*-quinone-H^+ were determined.

In this paper, we have studied the oxidation of another catecholamine, epinine (*N*-methyldopamine or deoxyepinephrine), which has been proved to produce dilation or contraction of the cerebral arteries depending on its localization [9]. It is a strong noncompetitive inhibitor of dihydropteridine reductase of human liver [10] but, on the

Correspondence address: F. García Cánovas, Departamento de Bioquímica, Facultad de Medicina, Universidad de Murcia. Murcia, Spain.

other hand, it stimulates the conversion of arachidonic acid into prostaglandin [11].

Spectroscopic analysis of the intermediates of this route up to epininechrome has been carried out following a methodology similar to that published in former papers [3,5–7]. However, the high rate of the chemical reaction coupled to an enzymatically catalyzed step may suppose an overlap in time between the transient phases corresponding to both reactions. Thus, in this paper, we have made a kinetic analysis of the overall transient phase, obtaining analytical expressions for situations in which some exponential terms are negligible.

On the other hand, data analysis, by nonlinear regression, has been applied to the progress curves, thereby allowing the rate constants, k_1', k_{-1}' and k_2', corresponding to the deprotonation, protonation and cyclization steps, respectively, to be calculated at different temperatures. Two new approaches, involving kinetic analysis of the transient phase and data analysis by nonlinear regression, together with a study of the route, have thus been carried out in the present paper.

2. Theory

The widely accepted model for tyrosinase reaction on *o*-diphenols is shown in scheme 1 [12], where the protonated quinonic product QH^+ undergoes a deprotonation reaction, followed by cyclization, the product of which is then oxidized by a molecule of QH^+ simultaneously causing both the regeneration of *o*-diphenol and formation of the corresponding aminochrome [4].

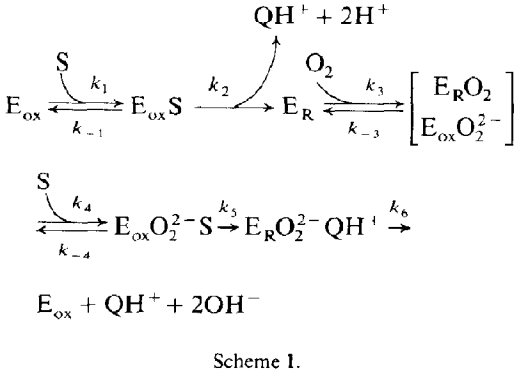

Scheme 1.

The species QH^+ follows a sequence of chemical reactions which are not enzymatically catalyzed. These reactions will henceforth be referred to as 'chemical reactions' and they are:

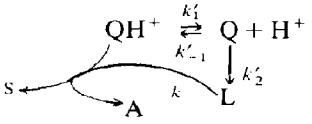

Scheme 2.

Notation and symbols:

E_{ox} or X_1 = oxidized enzyme; met-tyrosinase
$E_{ox}S$ or X_2 = met-tyrosinase/substrate complex
E_R or X_3 = reduced enzyme; deoxytyrosinase
$\begin{bmatrix} E_RO_2 \\ E_{ox}O_2^{2-} \end{bmatrix}$ or $X_4 = \begin{bmatrix} \text{deoxytyrosinase-} \\ \text{oxygen complex} \\ \text{oxytyrosinase} \end{bmatrix}$
$E_{ox}O_2^{2-}S$ or X_5 = oxytyrosinase-diphenol complex
$E_RO_2^{2-}QH^+$ or X_6 = intermediate complex with product
S or Y_1 = substrate, epinine
O_2 or Y_2 = substrate, oxygen
QH^+ or Y_3 = product, epininequinone-H^+
Q or Y_4 = epininequinone
L or Y_5 = leukoepininechrome
A or Y_6 = epininechrome
x_i = concentration of X_i species ($i = 1, 2, \ldots, 6$)
x_i^0 = concentration of X_i at $t = 0$ ($i = 1, 2, \ldots, 6$)
$\dot{x}_i = dx_i/dt$ ($i = 1, 2, \ldots, 6$)
y_j = concentration of Y_j species ($j = 1, 2, \ldots, 6$)
y_j^0 = concentration of Y_j at $t = 0$ ($j = 1, 2, \ldots, 6$)
$\dot{y}_j = dy_j/dt$ ($j = 1, 2, \ldots, 6$)

Initial conditions:

$x_1^0 = 0$
$y_1^0 \gg x_1^0$
$y_2^0 \gg x_1^0$
$y_j^0 = x_i^0 = 0 \quad (j = 3, 4, 5, 6;\ i = 2, 3, \ldots, 6)$

Differential equation system:

$$\dot{x}_1 = -k_1 y_1^0 x_1 + k_{-1} x_2 + k_6 x_6 \tag{1}$$

$$\dot{x}_2 = k_1 y_1^0 x_1 - (k_{-1} + k_2) x_2 \tag{2}$$

$$\dot{x}_3 = k_2 x_2 - k_3 y_2^0 x_3 + k_{-3} x_4 \tag{3}$$

$$\dot{x}_4 = k_3 y_2^0 x_3 - (k_{-3} + k_4 y_1^0) x_4 + k_{-4} x_5 \tag{4}$$

$$\dot{x}_5 = k_4 y_1^0 x_4 - (k_{-4} + k_5) x_5 \quad (5)$$

$$\dot{x}_6 = k_5 x_5 - k_6 x_6 \quad (6)$$

$$\dot{y}_3 = k_2 x_2 + k_6 x_6 + k'_{-1}[H^+] y_4 - k'_1 y_3 - k y_3 y_5 \quad (7)$$

$$\dot{y}_4 = k'_1 y_3 - (k'_{-1}[H^+] + k'_2) y_4 \quad (8)$$

$$\dot{y}_5 = k'_2 y_4 - k y_3 y_5 \quad (9)$$

$$\dot{y}_6 = k y_3 y_5 \quad (10)$$

2.1. General solution

The solution of the linear differential equation system consisting of eqs. 1–6 in accordance with ref. 13, leads to

$$x_2 = A_{20} + \sum_{h=1}^{5} A_{2h} \exp(\lambda_h t) \quad (11)$$

$$x_6 = A_{60} + \sum_{h=1}^{5} A_{6h} \exp(\lambda_h t) \quad (12)$$

A_{20}, A_{2h}, A_{60} and A_{6h} being defined in the appendix.

In turn, the λ_h ($h = 1, 2, \ldots, 5$) are the roots of the equation

$$\lambda^5 + M_1\lambda^4 + M_2\lambda^3 + M_3\lambda^2 + M_4\lambda + M_5 = 0 \quad (13)$$

M_1, M_2, M_3, M_4 and M_5 also being described in the appendix.

On the other hand, the differential equation system consisting of eqs. 7–10, is not linear. Thus, to resolve it analytically, we assumed that the Y_5 species is in the steady state from the beginning of the reaction, i.e., $\dot{y}_5 = 0$ and $y_5 \to 0$, as well as $k \to \infty$, so that the product $k y_3 y_5$ is not continuously zero. Thus, from eq. 9, $k'_2 y_4 = k y_3 y_5$. Taking into account in eq. 7 the anterior equality and eqs. 11 and 12, it results that the system consisting of eqs. 7 and 8 becomes linear and inhomogeneous, while eq. 10 can be written as:

$$\dot{y}_4 = k'_2 y_4 \quad (14)$$

The solution of the above-mentioned inhomogeneous system (eqs. 7 and 8) yields the expression of y_4 as a function of time which, when substituted into eq. 14, finally gives:

$$y_6 = y_E + y_Q \quad (15)$$

where

$$\begin{aligned} y_E = \Bigg\{ & \Bigg[\delta_2 (\delta_2 - \delta_1)^{-1} \\ & \times \exp(\delta_1 t) \Bigg(\sum_{h=1}^{5} \alpha_h (\lambda_h - \delta_1)^{-1} \Bigg) \Bigg] \\ & - \Bigg[\delta_1 (\delta_2 - \delta_1)^{-1} \\ & \times \exp(\delta_2 t) \Bigg(\sum_{h=1}^{5} \alpha_h (\lambda_h - \delta_2)^{-1} \Bigg) \Bigg] \\ & + \Bigg[\delta_1 \delta_2 \Bigg(\sum_{h=1}^{5} \alpha_h \lambda_h^{-1} (\lambda_h - \delta_1)^{-1} \\ & \times (\lambda_h - \delta_2)^{-1} \exp(\lambda_h t) \Bigg) \Bigg] \\ & - \Bigg[\sum_{h=1}^{5} \alpha_h \lambda_h^{-1} \Bigg] \Bigg\} / 2 \end{aligned} \quad (16)$$

and

$$\begin{aligned} y_Q = v_0 \{ & [(\delta_1 + \delta_2)/(\delta_1 \delta_2)] \\ & + t - [\delta_2 \exp(\delta_1 t)/(\delta_1 (\delta_2 - \delta_1))] \\ & + [\delta_1 \exp(\delta_2 t)/(\delta_2 (\delta_2 - \delta_1))] \} / 2 \end{aligned} \quad (17)$$

The parameters δ_1 and δ_2 verify the relations:

$$\delta_1 \delta_2 = 2 k'_1 k'_2 \quad (18)$$

$$\delta_1 + \delta_2 = -(k'_1 + k'_{-1}[H^+] + k'_2) \quad (19)$$

In turn, v_0 and α_h are given by:

$$v_0 = k_2 A_{20} + k_6 A_{60} \quad (20)$$

$$\alpha_h = k_2 A_{2h} + k_6 A_{6h} \quad (21)$$

Note that v_0 is the rate at which Y_3 is formed in the steady state, when no coupled reactions take place, as can be deduced from eqs. 7, 11 and 12.

Eq. 15 is the general expression describing the evolution of the Y_6 concentration in time. However, in real situations, there may be some particu-

lar cases which allow this general equation to be simplified. There now follows a discussion of such cases.

2.2. Particular cases

(a) When there is no overlap between the enzymatically catalyzed reaction and the sequence of chemical reactions, eq. 22 is valid:

$$\begin{aligned} &|\delta_1| \ll |\lambda_h| \quad (i=1,2;\ h=1,2,\ldots,5) \\ &|\lambda_h| \to \infty \quad (h=1,2,\ldots,5) \end{aligned} \tag{22}$$

Under these conditions, it is easy to show that, approximately, $y_E = 0$, so that eq. 15 can be simplified to

$$\begin{aligned} y_6 = v_0\Big\{\Big[&(\delta_1+\delta_2)(\delta_1\delta_2)^{-1}+t \\ &-\left[\delta_2\delta_1^{-1}(\delta_2-\delta_1)^{-1}\right)\exp(\delta_1 t)\Big] \\ &+\left[\delta_1\delta_2^{-1}(\delta_2-\delta_1)^{-1}\exp(\delta_2 t)\right]\Big\}/2 \end{aligned} \tag{23}$$

(b) When there is no overlap between the chemical and the enzymatically catalyzed reactions and, in the sequence of chemical reactions, the two exponentials are very different.

It can thus be established that

$$|\delta_1| \ll |\delta_2| \tag{24}$$

obtaining

$$y_6 = v_0\left\{t+\delta_1^{-1}\left[1-\exp(\delta_1 t)\right]\right\}/2 \tag{25}$$

Taking eqs. 19 and 24 into account, then

$$\delta_2 \simeq \delta_1+\delta_2 = -\left(k_1'+k_{-1}'[H^+]+k_2'\right) \tag{26}$$

Thus, from eq. 18, we deduce

$$-\delta_1 \simeq 2k_1'k_2'/\left(k_1'+k_{-1}'[H^+]+k_2'\right) \tag{27}$$

3. Materials and methods

Mushroom tyrosinase (monophenol monooxygenase, EC 1.14.18.1, 2230 units/mg) and epinine (*N*-methyldopamine or deoxyepinephrine) were purchased from Sigma. Sodium metaperiodate was analytical grade from Merck. Spectra were recorded using an Aminco DW-2 spectrophotometer with scanning speeds up to 20 nm/s. Reference cuvettes contained, in all cases, all the components except substrate. Oxygen consumption was followed with a Rank oxygen electrode (Rank Brothers). Temperature was controlled by using a Gilson bath and a digital Cole-Parmer thermistor to within ± 0.1°C.

Determination of the number of species formed in the chemical or enzymatic oxidations of epinine was based on the spectra obtained by application of the matrix analysis of Coleman et al. [14], using a Hewlett-Packard HP-85 computer.

The accumulation of epininechrome was followed spectrophotometrically at $\lambda = 475$ mm, $\epsilon = 3600\ M^{-1}\ cm^{-1}$; at this wavelength, neither substrate nor intermediate products were absorbed. The spectrophotometrical measurements were carried out using an Aminco DW-2 spectrophotometer equipped with stopped-flow accessory provided with two syringes. One syringe was filled with 3.6 mM epinine solution in acetate buffer at different pH and, the other, with an enzyme solution in distilled water, so that, with each shot, 50 μl from each syringe was released into the measuring compartment.

4. Results

In order to characterize the intermediates of the route of oxidation of epinine by tyrosinase and to determine whether such a route follows the sequence of an enzymatic-chemical-chemical mechanism (EzCC) with substrate regeneration, a series of assays of oxidation with periodate and enzyme were carried out. Firstly the possible intermediates, and the overall stoichiometry were detected, and then the rate constants involved were calculated.

4.1. Oxidation with sodium periodate

It is known that periodate oxidizes *o*-diphenols to give the corresponding *o*-quinones [15]; thus, this chemical model is similar to the reaction catalyzed by tyrosinase with respect to the reaction product. Epinine oxidation by sodium periodate was carried out at different [substrate]/[oxidant] ratios, as shown in fig. 1. A maximum was detected at $\lambda_{max} = 390$ nm that evolved with

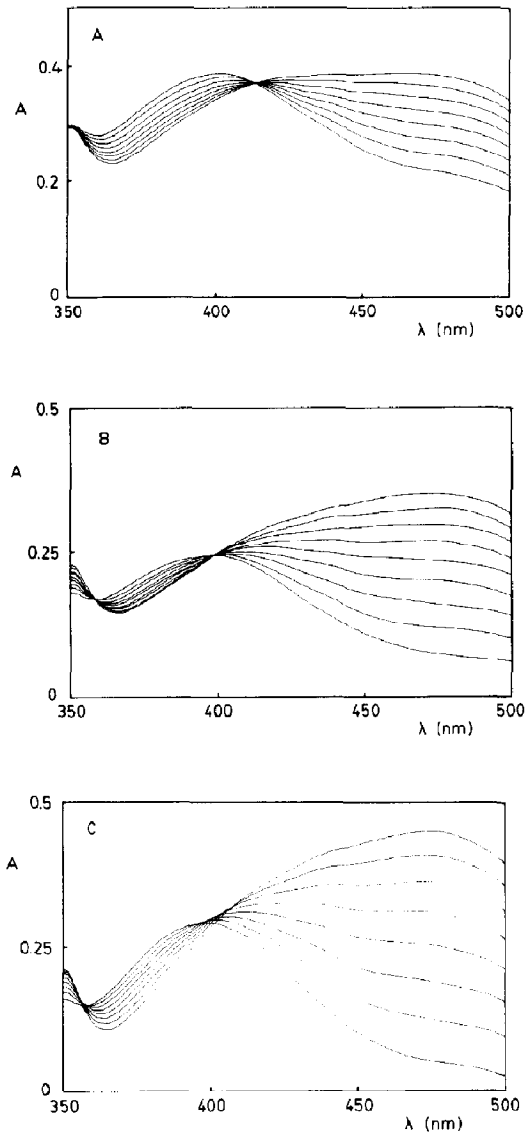

Fig. 1. Spectrophotometric recordings for the oxidation of epinine by sodium periodate at 12° C in 0.01 sodium acetate buffer, pH 3.8. Scan speed was up to 20 nm/s. (A) Epinine at 6.8 mM was oxidized with 0.36 mM $NaIO_4$. The first scan was started at 60 s from the beginning of the reaction and the others were recorded every 15 s. (B) Epinine at 0.23 mM was oxidized with 7.7 mM $NaIO_4$. The first scan was started at 45 s from the beginning of the reaction and the others were recorded every 15 s. (C) Epinine at 0.2 mM was oxidized with 0.2 mM $NaIO_4$. The first scan was started at 60 s from the beginning of the reaction and the others were recorded every 30 s.

time to $\lambda_{max} = 475$ nm. These two maxima, in agreement with Graham and Jeffs [16], were assigned to *o*-quinone (390 nm) and its respective aminochrome (475 nm). The formation of isosbestic points in fig. 1A and B, at $\lambda = 414$ and 398 nm, respectively, indicated that *o*-quinone was transformed into aminochrome at a constant ratio. Matrix analysis of the spectra in fig. 1A and B, by the method described in ref. 14, confirmed the presence of two kinetically related species (fig. 2A and B).

The recordings of fig. 1C were obtained when oxidation was carried out under equimolar conditions, viz., [epinine]/[oxidant] = 1. Under these conditions no isosbestic point appeared. Graphic analysis of the spectra showed three absorbing kinetically related species (fig. 2C).

When the concentration difference is high, the oxidation of *o*-diphenol by periodate is practically instantaneous. This proves useful in determining the stoichiometry between the generated *o*-quinone and its transformation into aminochrome. As shown in fig. 3, the maximal concentration of *o*-quinone, 0.5 mM ($\epsilon_{390} = 1040\ M^{-1}\,cm^{-1}$) (curve a), was reached immediately, this concentration being equal to that of the periodate added. The maximal concentration of aminochrome (curve b) was reached at 5 min and amounted to 0.24 mM ($\epsilon_{475} = 3600\ M^{-1}\,cm^{-1}$), this value being approximately half that of the periodate concentration. Since the concentration of periodate was fully consumed, this oxidation could be due to oxygen or to the *o*-quinone. However, oxygen consumption could not be detected in the course of the reaction (curve C of fig. 3). The oxidation of leukoaminochrome by its quinone can be explained by the difference in redox potential between *o*-quinone/*o*-diphenol and aminochrome/leukoaminochrome [17]. The above results suggest that *o*-quinone oxidizes the leuko compound, and is reduced in turn to epinine. To generate one aminochrome molecule, two *o*-quinone molecules are therefore necessary.

4.2. Oxidation by tyrosinase

Fig. 4 shows the visible spectra obtained for oxidation of epinine by mushroom tyrosinase. Two

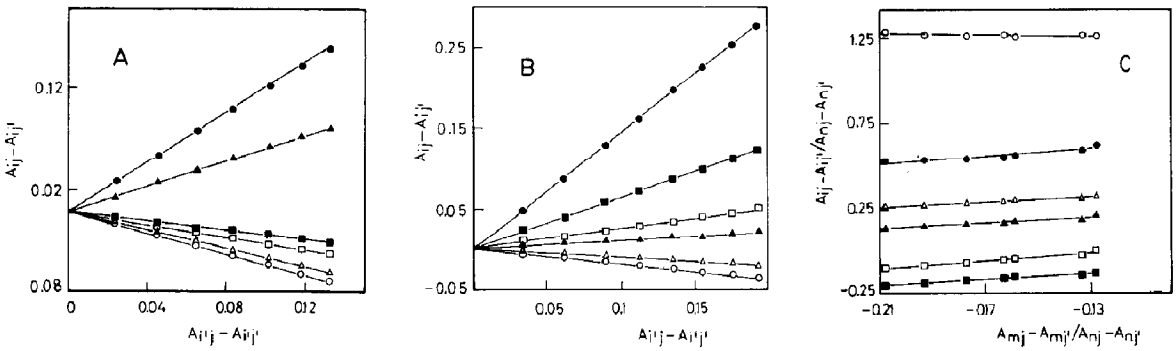

Fig. 2. Graphical analysis of spectra recorded during sodium periodate oxidation of epinine. Spectra were recorded at 20 nm/s. In this analysis, A_{ij} is the absorbance at wavelength i obtained during tracing j, so that A_{21} is the absorbance at 375 nm obtained during the first tracing of the absorption spectrum. (A) Graphical analysis of the spectra obtained when [epinine] > [$NaIO_4$] (fig. 1A). Selected wavelengths were: (□) 360 nm, (○) 375 nm, (△) 390 nm, (■) 406 nm, (▲) 436 nm, (●) 496 nm, $i' \equiv 440$ nm and $j' \equiv$ tracing 1. In both cases A and B, the matrix analysis for two species with restrictions was applied. (B) Graphical analysis of the spectra obtained when [epinine] < [$NaIO_4$] (fig. 1B). Selected wavelengths were: (▲) 355 nm, (○) 366 nm, (△) 392 nm, (□) 411 nm, (■) 425nm, (●) 478 nm, $i' \equiv 440$ nm and $j' \equiv$ tracing 1. (C) Graphical analysis of the spectra obtained when [epinine] = [$NaIO_4$] (fig. 1C). Selected wavelengths were: (▲) 352 nm, (■) 388 nm, (□) 395 nm, (△) 410 nm, (●) 425 nm, (○) 478 nm, $m \equiv 365$ nm, $n \equiv 448$ nm and $j' \equiv$ tracing 1. The test for three species with restrictions was applied.

maxima appeared at 390 and 475 nm, respectively, which were analogous to those in the oxidation with periodate (fig. 1). In these spectra, there are two different zones, the first consisting of tracings 1–10 and the second of 10–16, the latter having an isosbestic point at $\lambda = 410$ nm. This indicated that, as we had used a high concentration of tyrosinase, the enzymatically catalyzed reaction had stopped due to depletion of oxygen. Thus, recordings 10–16 corresponded to the chemical conversion of accumulated *o*-quinone-H^+ into its products. All spectra were subjected to graphic analysis [14] to determine the number of absorbing species in solution. The analysis of recordings 1–10 of fig. 4 fulfilled the test for three absorbing species in solution (results not shown). This situa-

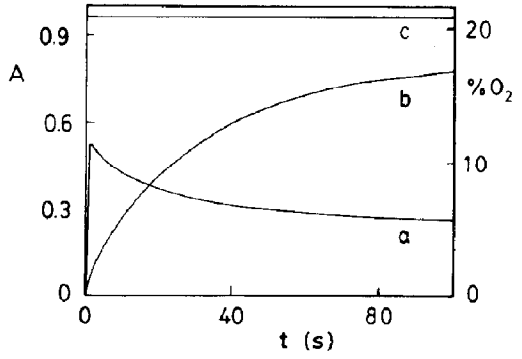

Fig. 3. Progress of the reaction for oxidation of 1.8 mM epinine with 0.5 mM $NaIO_4$, at pH 3.8 and 15°C. (a) A_{390} variation, (b) A_{475} variation, (c) oxygen determination.

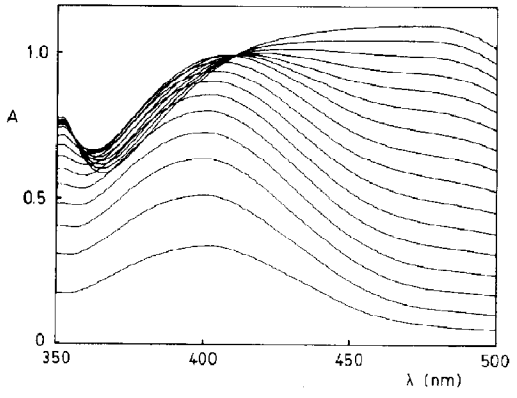

Fig. 4. Spectrophotometric recordings for the oxidation of 0.57 mM epinine by mushroom tyrosinase (2.9 mg/ml) at 12°C in 10 mM sodium acetate buffer, pH 3.8. Scan speed up to 20 nm/s. The first recording was started at 15 s from the beginning of the reaction.

tion is analogous to that of figs. 1C and 2C. From tracings 10–16 onwards, two kinetically related species were detected (data not shown). This situation is analogous to that of figs. 1A and 2A.

To establish the stoichiometry of enzymatic oxidation, an assay was performed by following the absorbance increase with reaction time at 390 and 475 nm, respectively (fig. 5). The rate of enzymatically catalyzed reaction was evaluated as the tangent, at $t = 0$, to the recording of absorbance at 390 nm (curve a) and as the slope of the linear zone of the aminochrome accumulation curve (curve b). The rate of *o*-quinone-H^+ production (36 μmol/min) was 2-fold greater than that of aminochrome accumulation (17 μmol/min). These results, together with those shown in the preceding figures, suggest a set of steps as shown in scheme 3, agreeing with the postulated pathway for L-dopa oxidation by tyrosinase [3].

4.3. Kinetic approximation

The accumulation of epininechrome by tyrosinase shows a lag period before reaching a constant accumulation rate (fig. 6A). The steady-state rate (measured as the slope in the linear zone of epininechrome accumulation) is linearly dependent on the enzyme concentration (fig. 6B) which is in agreement with eq. 15. On the other hand, the lag period (defined as the intercept on the abscissa of the tangent, at $t \to \infty$, to the epininechrome accumulation curve) was independent of enzyme concentration and had a value lower than 1 s at pH 4.8 and 20 °C. This requires the use of the stopped-flow technique for recording these kinetics and enables one to consider a possible overlap between the transient time corresponding to the enzymatically catalyzed reaction and that of the chemical reactions of the transformation of *o*-quinone-H^+ into epininechrome, as developed in section 2.

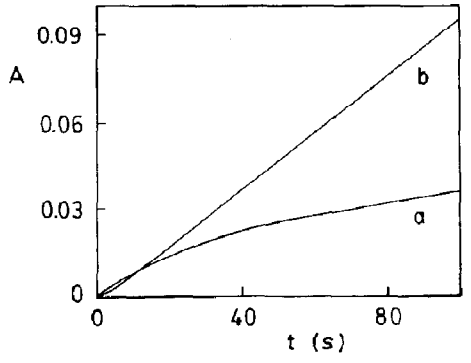

Fig. 5. Product formation as a function of time for 1.8 mM epinine oxidation with tyrosinase (16.6 μg/ml) at 15 °C and pH 4.8. (a) Absorbance increase with time at 390 nm; (b) absorbance increase of epininechrome accumulation at 475 nm.

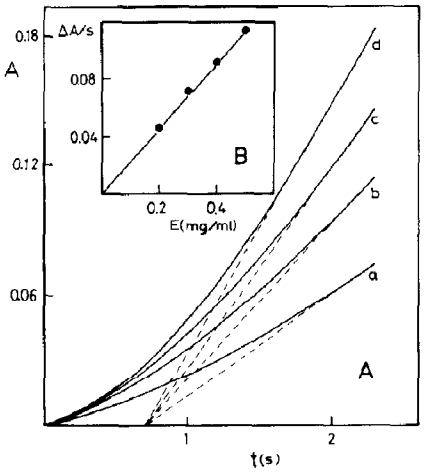

Fig. 6. (A) Epininechrome accumulation as a function of time at pH 4.8 and 20 °C followed by the absorbance increase at 475 nm for 1.8 mM epinine oxidation by different enzyme concentrations (μg/ml): (a) 0.2, (b) 0.3, (c) 0.4, (d) 0.5. (B) Plot of epininechrome accumulation rate under steady-state conditions vs. enzyme concentration.

The experimental data shown in fig. 6A are fitted by nonlinear regression [18] to eq. 25 and the corresponding values for the χ^2 statistic have been obtained. These values have been compared by using the F test [19] which makes it possible to determine objectively the equation that provides the best fit. The fit was always successful to a monoexponential equation, indicating that eq. 25 is sufficient to describe the experimental kinetic behavior (fig. 6A). This, therefore, means that there is no overlap between the enzymatically catalyzed reactions and the chemical reactions and that, in the transient time, only one chemical exponential (δ_1) is significant.

4.4. Effects of pH and temperature

Several series of kinetic assays at different values of pH and temperature have been carried out. The corresponding values of the parameters v_0 and δ_1, have been obtained by nonlinear regression of experimental data to eq. 25 [18]. The parameter $-\delta_1$ increases when pH and/or temperature rise (fig. 7). An additional fitting of $-\delta_1$ vs. $[H^+]$ data to eq. 27, using nonlinear regression [18], enables the specific rate constants to be calculated for the deprotonation steps from *o*-quinone-H^+ to *o*-quinone and for the inverse reaction, as well as for the cyclization from *o*-quinone to leukoaminochrome. This process has been performed at all chosen temperatures (fig. 7), the values of the respective rate constants as well as the corresponding estimations of their reliability being listed in table 1. The initial estimations of the rate constants for this data fitting have been determined by linear regression analysis of the corresponding $1/(-\delta_1)$ vs. $[H^+]$ data, using the characteristic pK_a value of the methylamine group of epinine [20]. The values of $-\delta_1$ calculated using these values of the rate constants do not agree well with the original values of this parameter (data not shown). However, the values of $-\delta_1$ calculated using the values of the rate constants obtained by nonlinear regression show the best overlap with the original values of this parameter (see fig. 7).

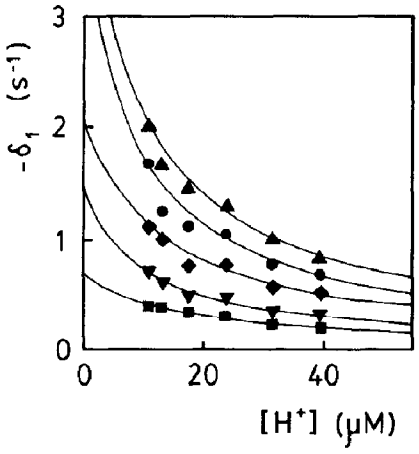

Fig. 7. Dependence of $-\delta_1$ on $[H^+]$ at several temperatures. Values of $-\delta_1$ were calculated using eq. 25 as described in section 4. Assay conditions were 0.4 μg/ml tyrosinase, 1.8 mM epinine at several temperatures (°C): (■) 20, (▼) 25, (◆) 30, (●) 35, (▲) 40. Other conditions as described in section 3. (———) Values calculated using the final estimations of rate constants from the nonlinear regression analysis to eq. 27.

Arrhenius plots (data not shown) were made using the previously obtained k_1', k_{-1}' and k_2' values, for the calculation of the activation energies. Later on, the corresponding activation parameters summarized in table 2, were calculated.

Table 1

Values of rate constants at various temperatures

Values of the first-order rate constants for deprotonation of epininequinone-H^+ to epininequinone (k_1'), the second-order rate constant of the inverse process (k_{-1}') and for the cyclization of epininequinone to leukoaminochrome (k_2') at various temperatures are listed.

T (°C)	k_1' (s^{-1})	k_{-1}' ($M^{-1}\,s^{-1}$) ($\times 10^{-10}$)	k_2' (s^{-1}) ($\times 10^{-6}$)
20	0.34 ± 0.02	2.83 ± 0.19	0.48 ± 0.03
25	0.73 ± 0.04	5.78 ± 0.38	0.59 ± 0.04
30	1.04 ± 0.06	8.25 ± 0.56	1.06 ± 0.07
35	1.86 ± 0.10	14.09 ± 0.97	1.22 ± 0.09
40	2.10 ± 0.12	16.56 ± 1.09	1.64 ± 0.12

Table 2

Values of the thermodynamic parameters

Thermodynamic activation parameters for the deprotonation of epininequinone-H^+ into *o*-epininequinone, the inverse process and the cyclization of epininequinone to leukoepininechrome are given.

Step	E_a (kJ mol^{-1})	$\Delta H^{\ddagger}$ (kJ mol^{-1})	$\Delta G^{\ddagger}$ (kJ mol^{-1})	$\Delta S^{\ddagger}$ (J K^{-1} mol^{-1})
Deprotonation	66.2 ± 5.3	63.7 ± 5.1	72.4 ± 5.9	−29.2 ± 2.4
Protonation	80.1 ± 7.1	77.7 ± 7.2	13.1 ± 1.2	220.4 ± 19.7
Cyclization	49.7 ± 5.1	47.2 ± 4.7	39.9 ± 4.1	24.4 ± 2.5

5. Discussion

The oxidation of epinine by tyrosinase should follow the same mechanism as that proposed for different catecholamines [3–8], the appearance of a quinonic form ($\lambda = 390$ nm) being detected at acid pH with both sodium periodate and enzyme (figs. 1 and 4).

The cyclization of the quinonic to the leuko form follows the intramolecular addition 1–4 of Michael. This cyclization is only possible when the methylamine group is deprotonated. The reaction therefore depends on pH, as shown in scheme 3. Thus, for pH values lower than 5, the apparent cyclization constant becomes smaller, thereby enabling spectrophotometric detection of the quinonic form. In scheme 3, both a protonated and a deprotonated quinonic form in solution can be seen. The values of the constants of both deprotonation and cyclization, as well as their corresponding $t_{1/2}$ values, indicate that the protonated form is the most abundant in solution. Comparison of the above constants with those of dopamine [5] shows the lower stability of *o*-epininequinone-H^+ with respect to *o*-dopaminequinone-H^+. This suggests that the presence of the

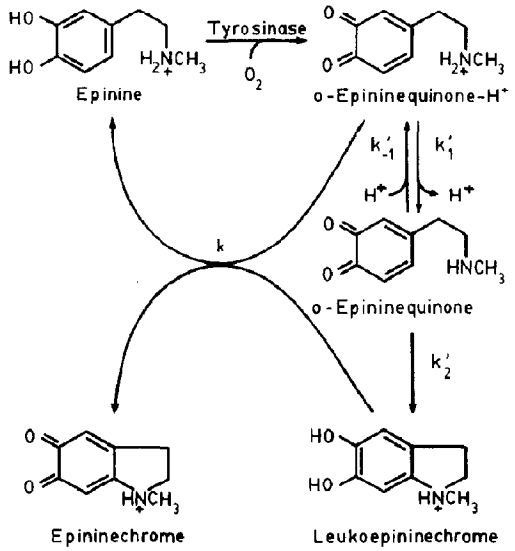

Scheme 3.

methyl group, due to its inductive character (+I), facilitates the cyclization reaction; with epinine it is thus necessary to work with a more acidic pH than with dopamine.

In fig. 4, from tracing 10, the transformation without oxygen of *o*-quinone-H^+ into aminochrome can be observed, all O_2 having previously been consumed. The assays with sodium periodate show that the rate of accumulation of aminochrome is half that of *o*-quinone-H^+ (fig. 3). The following stoichiometry can therefore be proposed:

2 *o*-epininequinone-H^+ → aminochrome + epinine

The absence of oxygen consumption in fig. 3 indicates that the leukoaminochrome oxidation is carried out by the *o*-quinone-H^+. In the initial moments, graphic analysis of the spectra of fig. 4 (results not shown) fulfills the test for three species, indicating the presence of three kinetically related species: epinine, *o*-epininequinone-H^+ and epininechrome. From tracing 10 onwards, the appearance of two isosbestic points indicates that there are two absorbing species. However, from the above considerations, it can be deduced that there are, in fact, three kinetically related species. Effectively, every two molecules of *o*-quinone-H^+ generate one molecule of leukoaminochrome, the latter, since there is no oxygen, being oxidized into aminochrome by the other molecule of *o*-quinone-H^+, thereby regenerating epinine. As aminochrome and epinine are formed in a constant relation with time, graphic analysis detects them as one. The same result is obtained when the epinine concentration is higher than that of sodium periodate (fig. 1A), an isosbestic point being observed at $\lambda = 410$ nm similar to the point in fig. 4. In fig. 1A, the matrix analysis also detected two kinetically related species but (fig. 2A), as mentioned above, there are three: epinine, *o*-quinone-H^+ and aminochrome.

The assays carried out with excess sodium periodate (fig. 1B) show, unlike fig. 1A, an isosbestic point at $\lambda = 398$ nm different from that of fig. 1A. This may be explained by the transformation of *o*-quinone-H^+ into aminochrome, following a stoichiometry of 1 : 1. Excess periodate impedes the accumulation of epinine in the medium and,

since excess periodate oxidizes leukoaminochrome, prevents oxidation of leukoaminochrome by *o*-quinone-H^+. Graphic analysis of fig. 1B fulfills the test for two species best, *o*-quinone-H^+ and aminochrome being demonstrated (fig. 2B).

When oxidation of epinine by periodate is carried out under equimolar conditions (fig. 1C), the oxidation and cyclization reactions take place at the same time, graphic analysis fulfilling the test for three species: epinine, *o*-quinone-H^+ and aminochrome (fig. 2C). The same result was obtained in tracings 1–10 of fig. 4.

The results obtained in the kinetic study show a good correspondence to the theoretical approximation that was applied to solve the kinetics of a chemical reaction system coupled to an enzymatically catalyzed step. This kinetic study also confirms that epinine oxidation into its aminochrome follows the same pathway previously proposed for other catecholamines [3–8] and also establishes that epininequinone-H^+ is less stable than *o*-dopaminequinone-H^+ at physiologic pH.

Analogously to our studies carried out with other catecholamines [3–8], the high rate of ring closure may, therefore, be attributed to a very favorable probability factor, as indicated by the high positive activation entropy.

In short, in this paper a general kinetic study for a chemical reaction system coupled to an enzymatically catalyzed step is presented. The particular cases in which there is no overlap between the two processes are discussed and an analysis by nonlinear regression is applied to calculate the rate constants involved in the chemical steps.

Appendix

$$M_1 = k_{-1} + k_{-3} + k_{-4} + k_2 + k_5 + k_6 + (k_1 + k_4)y_1^0 + k_3 y_2 \quad \text{(A1)}$$

$$M_2 = (k_{-1} + k_2)(k_{-3} + k_{-4} + k_5 + k_6) + k_{-3}(k_{-4} + k_5 + k_6) + (k_{-4} + k_5)k_6 + \left[k_1(k_{-3} + k_{-4} + k_2 + k_5 + k_6) + k_4(k_{-1} + k_2 + k_5 + k_6)\right] y_1^0 + k_3(k_{-1} + k_{-4} + k_2 + k_5 + k_6) y_2^0 + k_1 k_4 (y_1^0)^2 + k_3(k_1 + k_4) y_1^0 y_2^0 \quad \text{(A2)}$$

$$M_3 = (k_{-1} + k_2)\left[(k_{-4} + k_5)(k_{-3} + k_6) + k_{-3}k_6\right] + k_{-3}k_6(k_4 + k_5) + \left\{k_1\left[k_2 k_{-3} + k_2(k_{-4} + k_5) + k_2 k_6 + k_{-3}(k_{-4} + k_5) + k_6(k_{-3} + k_{-4} + k_5)\right] + k_4\left[k_5(k_{-1} + k_2) + k_6(k_{-1} + k_2) + k_5 k_6\right]\right\} y_1^0 + k_3\left[(k_{-1} + k_2)(k_{-4} + k_5) + k_6(k_{-1} + k_2) + k_6(k_{-4} + k_5)\right] y_2^0 + k_1 k_4(k_2 + k_5 + k_6) \times (y_1^0)^2 + \left[k_1 k_3(k_2 + k_{-4} + k_5 + k_6) + k_3 k_4(k_{-1} + k_2 + k_5 + k_6)\right] y_1^0 y_2^0 + k_1 k_3 k_4 (y_1^0)^2 y_2^0 \quad \text{(A3)}$$

$$M_4 = k_{-3}(k_{-1} + k_2)(k_{-4} + k_5)k_6 + \left\{k_1\left[k_2 k_{-3}(k_{-4} + k_5) + k_2 k_{-3} k_6 + k_2 k_6(k_{-4} + k_5) + k_{-3}k_6(k_{-4} + k_5)\right] + (k_{-1} + k_2)k_4 k_5 k_6\right\} y_1^0 + k_3 k_6(k_{-1} + k_2) \times (k_{-4} + k_5) y_2^0 + k_1 k_4(k_2 k_5 + k_2 k_6 + k_5 k_6) \times (y_1^0)^2 + k_3\left\{k_1\left[k_2(k_{-4} + k_5) + k_2 k_6 + (k_{-4} + k_5)k_6\right] + k_4\left[k_5(k_{-1} + k_2) + k_6 \times (k_{-1} + k_2) + k_5 k_6\right]\right\} y_1^0 y_2^0 + k_1 k_3 k_4(k_2 + k_5 + k_6)(y_1^0)^2 y_2^0 \quad \text{(A4)}$$

$$M_5 = k_1 k_2 k_6 k_{-3}(k_{-4} + k_5) y_1^0 + k_1 k_2 k_4 k_5 k_6 (y_1^0)^2 + \left[k_1 k_2 k_3(k_{-4} + k_5)k_6 + k_3 k_4 k_5 k_6(k_{-1} + k_2)\right] y_1^0 y_2^0 + k_1 k_3 k_4(k_2 k_5 + k_2 k_6 + k_5 k_6)(y_1^0)^2 y_2^0 \quad \text{(A5)}$$

$$A_{20} = k_1 k_3 k_4 k_5 k_6 (y_1^0)^2 y_2^0 x_1^0 / M_5 \quad \text{(A6)}$$

$$A_{60} = k_1 k_2 k_3 k_4 k_5 (y_1^0)^2 y_2^0 x_1^0 / M_5 \quad \text{(A7)}$$

$$A_{2h} = \left(a_0 + a_1\lambda_h + a_2\lambda_h^2 + a_3\lambda_h^3 + a_4\lambda_h^4\right) x_1^0 \Big/ \left[\lambda_h \prod_{\substack{p=1 \\ p\neq h}}^{5} (\lambda_p - \lambda_h)\right] \quad \text{(A8)}$$

$$a_0 = k_1k_3k_4k_5k_6\left(y_1^0\right)^2 y_2^0 \quad \text{(A9)}$$

$$a_1 = k_1k_3k_6(k_{-4} + k_5)\, y_1^0y_2^0 + k_{-3}k_1k_6(k_{-4} + k_5)\, y_1^0 + k_1k_4k_5k_6\left(y_1^0\right)^2 + k_1k_3k_4(k_5 + k_6)\left(y_1^0\right)^2 y_2^0 \quad \text{(A10)}$$

$$a_2 = k_1\left[k_6(k_{-4} + k_5) + k_{-3}(k_6 + k_{-4} + k_5)\right] y_1^0 + k_1k_3(k_{-4} + k_5 + k_6)\, y_1^0y_2^0 + k_1k_4(k_5 + k_6)\left(y_1^0\right)^2 \quad \text{(A11)}$$

$$a_3 = k_1(k_{-3} + k_{-4} + k_5 + k_6)\, y_1^0 + k_1k_3y_1^0y_2^0 + k_1k_4\left(y_1^0\right)^2 \quad \text{(A12)}$$

$$a_4 = k_1y_1^0 \quad \text{(A13)}$$

$$A_{6h} = k_1k_2k_3k_4k_5\left(y_1^0\right)^2 y_2^0x_1^0 \Big/ \left[\lambda_h \prod_{\substack{p=1 \\ p\neq h}}^{5} (\lambda_p - \lambda_h)\right] \quad \text{(A14)}$$

Acknowledgements

This work has been partially supported by a grant from the CAICYT (Spain), Project no. 0276/82. We acknowledge with thanks Dr. J. García De La Torre for critical reading of this article and Mrs. Stephanie Tischer for typing the manuscript.

References

1 T.B. Fitzpatrick, W.C. Quevedo, G. Szabo and M. Seiji, in: Dermatology in general medicine, ed. T.B. Fitzpatrick (McGraw-Hill, New York, 1971) p. 117.
2 W.H. Harrison, R.M. Gray and L.M. Salomon, Acta Derm.-Venereol. 54 (1974) 249.
3 F. García Cánovas, F. Carcia Carmona, J. Vera, J.L. Iborra and J.A. Lozano, J. Biol. Chem. 257 (1982) 8738.
4 F. García Garmona, F. García Cánovas, J.L. Iborra and J.A. Lozano, Biochim. Biophys. Acta 717 (1982) 124.
5 M. Jiménez, F. García Carmona, F. García Cánovas, J.L. Iborra, J.A. Lozano and F. Martinez, Arch. Biochem. Biophys. 235 (1984) 438.
6 M. Jiménez, F. García Cánovas, F. García Carmona, J.L. Iborra and J.A. Lozano, Biochem. Pharmacol. 11 (1985) 51.
7 M. Jiménez, F. García Carmona, F. García Cánovas, J.L. Iborra and J.A. Lozano, Int. J. Biochem. 17 (1985) 885.
8 M. Jiménez, F. García Carmona, F. García Cánovas, J.L. Iborra and J.A. Lozano, Int. J. Biochem. 17 (1985) 891.
9 J. McCulloch, Alpha-blockers, Symp. Int. 1979 (Masson, Paris, 1981) p. 331.
10 R.S. Shen, Biochim. Biophys. Acta 743 (1983) 129.
11 A.A. Abdel-Latif, J.P. Smith, S.Y.K. Jonsufzai and R.K. Dover, in: Proc. Int. Symp. Neural Membranes 1982, ed. G. Sun (Clifton, New York, 1983) p. 97.
12 K. Lerch, in: Metal ions in biological systems, ed. H. Sigel (Marcel Dekker, New York, 1981) vol. 13, p. 143.
13 J. Gálvez and R. Varón, J. Theor. Biol. 89 (1981) 1.
14 J.S. Coleman, L.P. Varga and S.H. Mastin, Inorg. Chem. 252 (1977) 5729.
15 S.W. Weidman and E.T. Kaiser, J. Am. Chem. Soc. 88 (1966) 5820.
16 D.G. Graham and P.W. Jeffs, J. Biol. Chem. 252 (1977) 5729.
17 G.A. Swan, Fortschr. Chem. Org. Naturst. 31 (1974) 521.
18 D.W. Marquardt, J. Soc. Ind. Appl. Math. 11 (1963) 431.
19 B. Mannervik, in: Kinetic data analysis, ed. L. Endrenyi (Plenum Press, New York, 1981) p. 235.
20 G.P. Lewis, Br. J. Pharmacol. 9 (1954) 488.